Cross-linked PEG Membranes of Interpenetrating Networks with Ionic Liquids as Additives for Enhanced CO_2 Separation

*Jing Deng, Junbo Yu, Zhongde Dai, Liyuan Deng**

Department of Chemical Engineering, Norwegian University of Science & Technology, 7491 Trondheim, Norway

KEYWORDS:

Click reactions; interpenetrating networks; PEG-based membrane; CO_2 separation; ionic liquids

ABSTRACT:

Polyethylene glycol (PEG)-based membranes have recently been reported with excellent CO_2 separation performances. However, the commonly exhibited high crystallinity may deteriorate the gas permeation properties in this type of membranes. In this work, a two-stage cross-linking method was employed to fabricate PEG membranes with interpenetrating networks to reduce the crystallinity. Ionic liquids (ILs) were incorporated into the resultant membranes to increase the diffusivity and the CO_2 affinity of the membranes. By increasing the length of the PEG-based acrylate monomers and optimizing the ratio of the amine cross-linker to the acrylate monomers, CO_2 permeability of the resultant membranes was significantly enhanced (from 0.6 to 85.0 Barrer) with slightly increased CO_2/N_2 selectivity. Four conventional ILs (i.e., [Bmim][BF_4], [Bmim][PF_6], [Bmim][NTf_2], and [Bmim][TCM]) with different anions were added into the optimized cross-linked PEG membranes. The addition of ILs endows superior gas transport properties at high loadings and the [Bmim][TCM] gives the best CO_2 separation performance of the membranes; CO_2 permeability of up to 134.2 Barrer with the CO_2/N_2 selectivity of 49.5 was documented. The anions in ILs were found contributing the most in promoting the CO_2 permeation, and the higher CO_2 affinity endows the better CO_2 separation performance in the resultant membranes.

1 Introduction

The membrane-based CO_2 capture technology, especially the use of polymeric membranes, has attracted widespread interest for its remarkable advantages, including low operation cost, high energy efficiency, easy scale-up or scale-down, and small footprint [1]. However, the CO_2 separation properties of current polymeric membrane materials are still not sufficient to make membrane technology competitive to the mature amine-absorption processes. According to the solution-diffusion mechanism involved in most polymeric membranes, two approaches could be taken to improve the separation performance of a polymeric membrane: to increase the CO_2 solubility (such as by introducing CO_2-philic moieties) or/and CO_2 diffusivity (e.g., through enlarging the free volume of the membrane matrices) [2, 3]. For the first approach, ether group (-C-O-) is a well-known functional group with high CO_2-philicity, hence polymers containing plenty ether groups, such as poly(ethylene glycol) (PEG, or also called poly(ethylene oxide) (PEO) at a high molecular weight), are expected to possess excellent CO_2 separation performance [2, 4-6].

However, the pristine PEO membranes were reported exhibiting very low CO_2 permeability (~ 10 Barrer) [7], most probably due to its high crystallinity resulted from its abundant ethylene oxide (EO) groups and the strong hydrogen bonding, which impedes gas transport through the membranes. It is reported that the formation of crystalline zones in PEO polymers requires 4 chains containing 7 EO units [3], and therefore the crystallinity could be suppressed via cross-linking PEG monomers with short chains by disrupting the repetition of PEG chains. Following this idea, Lin et al. reported that by simply cross-linking PEG diacrylate (PEGDA), the CO_2 permeability of the membrane increases by around 10-fold without sacrificing the CO_2 selectivity [8]. The greatly reduced

crystallinity and thus increased amorphous PEG phase release the restricted crystalline zone for gas diffusion, resulting in greatly improved CO_2 transport properties.

In addition, the length of the EO units or PEG monomers, which can be simply presented by their molecular weight (MW), is critical in determining the crystallinity and thus the final gas transport properties of the PEG-based membrane, as long polymer chains may result in increased crystalline zones. However, after crosslinking, the membranes prepared by monomers of long chains are more flexible and have more free volume for gas diffusion. Patel et.al cross-linked PEGDA membranes and reported that the CO_2 permeability increases significantly with the number of EO units in PEGDA [9]. The longer PEG monomers would result in much higher CO_2 diffusivity after cross-linking compared with those with short chains [10]. In addition to the enhancement in gas diffusivity, the EO density in membranes also slightly increases, leading to a simultaneous increment in CO_2 solubility. Hence, by simply employing longer PEG monomers, the consequent increase in both diffusivity and solubility generates a great increment (~10-fold) in CO_2 permeability. However, crystalline phases may form in polymers with the chain length of > 1500 g/mol [3], hence crosslinking with monomers of too long PEG chains may not be able to suppress the high crystallinity of the PEG polymers. On the other hand, crosslinking with monomers of short chains results in high cross-link density, leading to a low free volume of the polymer and low gas permeation. It is thus important to investigate the effects of the chain length in cross-linked PEG-based membranes to optimize the gas separation performance of the membranes.

The incorporation of low-molecular-weight "free" PEG into the PEG-based membranes has also been widely reported as an effective approach to reduce the crystallinity and increase the chain flexibility (and thus the free volume) of the polymers, which enhances the gas transport properties in membranes without sacrificing their CO_2 selectivity [11, 12]. Similarly, the addition of ionic liquids

(ILs) have been reported in improving the CO_2 permeability of membranes made of crystalline polymers [13-18]. ILs have been widely reported as CO_2-philic additives to improve the CO_2 separation performance of membranes in recent years [13, 19], especially for membranes of highly crystalline [15, 16, 20] or highly cross-linked polymers [21, 22]. The addition of ILs may reduce the crystallinity and increase the CO_2 diffusivity, therefore increase greatly the CO_2 permeation properties. Moreover, the high CO_2 affinity and the extremely low vapor pressure of ILs are the additional advantages as additives. Bara et al. [23] added only 20 mol% [Bmim][NTf_2] into poly(RTIL) membrane and the CO_2 permeability obtains remarkable enhancement (~ 4-fold) with a slight improvement in CO_2/N_2 selectivity (33%) compared with the pristine poly(RTIL) membrane. The addition of low viscosity [Emim][$B(CN)_4$] endows an excellent CO_2 permeability of 1778 Barrer (0.74 Barrer in its analog), and this great increment is mainly contributed by the increase in CO_2 diffusivity [15]. In addition, the tunable chemical structures of ILs give it more possibility to improve the membrane properties for diverse requirements [24]. However, some research works reported that the addition of ILs into polymeric materials did not result in an expected gain in gas permeability [25, 26]. It is believed that the compatibility between ILs and the polymeric matric have the decisive influence on the final performance.

Despite of the similar role between ILs and PEG materials, the combination of these two approaches is rarely studied in CO_2 separation membranes. In this work, the incorporation of ILs into the cross-linked PEG-based membranes has been systemically investigated. Firstly, a series of cross-linked PEG-based membranes with interpenetrating polymeric networks was fabricated through a facile, two-stage cross-linking method based on aza-Michael addition and acrylate homopolymerization [27, 28]. The cross-linking density of the resultant PEG membranes was optimized by controlling the molecular weight of the acrylate-functionalized PEG-based monomer

and the ratio of amine cross-linkers to acrylate monomers. The influences on the chemical structure, thermal properties, phase transition behavior, crystalline trend and gas permeation properties were studied by various characterization techniques. Moreover, four conventional ILs with the same cation $[Bmim]^+$ but different anions were incorporated into the optimized cross-linked PEG membranes, and their influences on the material properties and the gas separation performance were systemically investigated.

2 Experiment

2.1.Material

PEGDA with different molecular weight (250, 575 and 700 g/mol), tris(2-aminoethyl)amine (TAEA), 1-hydroxycyclohexyl phenyl ketone (HCPK) and three ionic liquids 1-butyl-3-methylimidazolium bis(trifluoromethylsulfonyl)imide ([Bmim][NTf_2], 98%), 1-butyl-3-methylimidazolium tetrafluorobotate ([Bmim][BF_4], 98%) and 1-butyl-3-methylimidazolium hexafluorophosphate ([Bmim][PF_6], 98%) were purchased from Sigma-Aldrich, Germany. 1-butyl-3-methylimidazolium tricyanomethanide ([Bmim][TCM], 98%) was ordered from Iolitec, Germany. The N_2 and CO_2 gases (99.999%) used in the single gas permeation test were provided by AGA, Norway. The chemical structures of the above-mentioned chemicals were depicted in Fig.1.

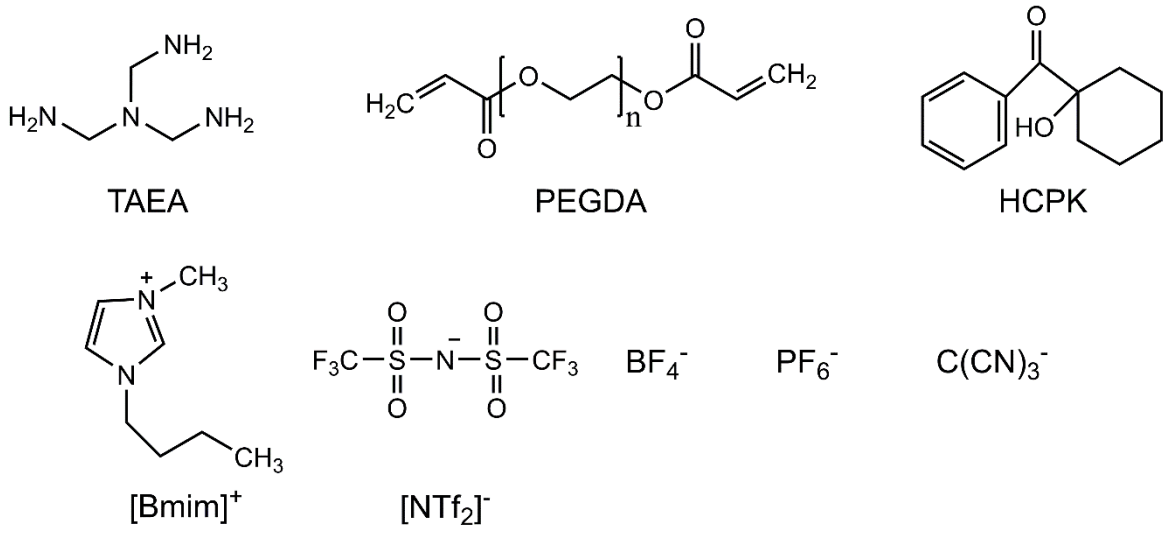

Figure 1 Chemical structures of all chemicals used in the current work

2.2.Membrane preparation

The cross-linked PEG membranes were prepared through a two-stage method similar to that reported in the literature [11, 27, 28]. For the readers' convenience, a brief description is presented below. Firstly, monomer PEGDA, the desired amount of ionic liquid, and photoinitiator HCPK (0.01 ~ 0.1 wt% of PEGDA) were magnetically mixed inside a glass vial for 30 minutes at room temperature (R.T.). Then proper amount of the cross-linker TAEA was added into the resultant homogeneous mixture and magnetically stirred (~ 30 minutes, R.T.) to ensure a complete reaction (aza-Michael addition) between amine and acrylate. Afterwards, , the mixtures were degassed in a vacuum oven for a few minutes at R.T. to remove the possible bubbles. The mixture was then poured onto a clean quartz plate and sandwiched by using a second quartz plate on the top. The plates were separated by several spacers to control the membrane thickness (200 ~ 250 μm). The liquid mixture was exposed under UV light with a wavelength of 365 nm for 2 hours (UVLS-28, Ultra-Violet Products Ltd., UK) for the homo-polymerization of excess acrylate. After irradiation, the cross-linked membranes were transferred to a vacuum oven overnight at 60 ^{o}C before further characterization. These membranes were evaluated by various characterization methods and permeation tests. The mass ratio of ILs is defined as the mass of ionic liquid over PEGDA, as shown in Equation 1:

$$W_{IL} = \frac{m_{IL}}{m_{PEGDA}} \times 100\% \quad (1)$$

In this work, the cross-linked PEG membranes are systematically designated as "TAEA-PEGDA XX-X-X" according to the ratio of amine-containing cross-linker (TAEA) to acrylate-terminated monomer (PEGDA with a molecular weight of XX g/mol). For example, the TAEA-PEGDA 700-1-6 membrane consists of TAEA and PEGDA (MW 700 g/mol) with 1 N-H bond from TAEA and 6 acrylate groups from PEGDA 700.

2.3. Characterization

A Thermo Nicolet Nexus Fourier-transform infrared spectrometer (FT-IR, Oslo, Norway) with an attenuated total reflectance (ATR) cell equipped with a diamond crystal was used to collect the FT-IR spectra for all the membranes. Spectra were averaged over 16 scans at a wavenumber resolution of 4 cm^{-1} in the range of 650 cm^{-1} to 4000 cm^{-1}. Small membrane samples were employed for FTIR tests and at least two spectra were collected for each membranes for the reproducibility and the uniformity of the membranes.

The thermal stability of the membranes was interrogated by thermogravimetric analysis (TGA) performed on a Thermal Scientific Q500 instrument, USA. Approximately 10 ~ 20 mg samples were heated in a ceramic crucible from 25 to 700 °C at a constant heating rate of 10 °C/min under N_2 to prevent thermo-oxidative degradation of the samples.

A differential scanning calorimeter (DSC, DSC 214 Polyma, NETZSCH-Gerätebau GmbH, Germany) was used to investigate the phase transition behavior of all membranes. Samples with around 10 mg were collected in a standard aluminum pan covered by a proper lid and heated at the rate of 10 °C/min under N_2 atmosphere. Two cycles have been applied for the DSC tests and the curves from the second cooling run are used for further analysis.

The crystallinity of all membrane samples was examined by X-ray diffraction analysis (XRD) using a Bruker D8 A25 DaVinci X-ray Diffractometer, (Cambridge, UK). The XRD patterns were recorded from 5° to 70°.

2.4. Gas permeation test

The gas permeability (P) of both CO_2 and N_2 through the membranes was measured by the constant-volume variable-pressure method, which can be calculated based on equation (2):

$$P = \left[\left(\frac{dp_d}{dt}\right)_{t\to\infty} - \left(\frac{dp_d}{dt}\right)_{t\to leak}\right] \cdot \frac{V_d}{A \cdot R \cdot T} \cdot \frac{l}{(p_u - p_d)} \qquad (2)$$

where p_d and p_u identify the downstream and upstream gas pressures, respectively, and t is time. Here, V_d is the downstream volume, A corresponds to the effective permeation area of the membrane, R is the universal gas constant, T denotes absolute temperature, and l is the membrane thickness. The leakage rate of the gas permeation setup $(^{dp_d}/_{dt})_{t\to leak}$ was measured from the increase in pressure relative to vacuum over time. Membrane thicknesses were measured by a Digitix II thickness gauge. The thicknesses were averaged from more than 10 measurements for each membrane after permeation tests. All gas permeation experiments were performed using an upstream pressure of 2 bar (absolute) at room temperature. For each membrane, the reported permeabilities were the average of measurements acquired from at least two specimens. The ideal CO_2/N_2 selectivity was calculated from the ratio of gas permeabilities in accord with

$$\alpha_{ij} = \frac{P_i}{P_j} \qquad (3)$$

3 Result and discussion

3.1.Effect of PEGDA molecular weight

In this work, the effect of the length, or more precisely, MW, of the monomer PEGDA was systematically investigated. PEGDA of three different MW (250, 575 and 700 g/mol) has been employed to fabricate the membranes with dual cross-linking networks based on the aza-Michael reaction and the homo-polymerization of excess acrylate, as schemed in Scheme 1. It is worth mentioning that the MW of PEGDA is limited to < 1000 g/mol in order to reduce the formation of the crystalline phases. To confirm the two above-mentioned reactions, FI-TR analysis was employed to examine the monomers (PEGDA and TAEA), the product of the aza-Michael reaction (the mixture of PEGDA and TAEA with excess PEGDA), and the formed membranes (the ratio of N-H/acrylate is 1:6). As it can be seen in Fig. 2(A), the peaks related to amine groups (~ 3366 and 3265 cm^{-1}) disappear after mixing at R.T., and the peaks corresponding to acrylate (1635 and

1407 cm^{-1}) clearly show a reduced trend. These results imply that the amine and part of the acrylate react (aza-Michael addition) and form an N-H/acrylate cross-linking network because of the multi-functionalized TAEA. After UV irradiation, however, the remaining acrylate is hardly observed in all spectra of the formed membranes, regardless the MW of the used PEGDA, due to the homo-polymerization of PEGDA, which is known to have built cross-linking networks. Therefore, the network built by acrylate homo-polymerization as well as the interpenetrating structures inside the resultant membranes can be confirmed.

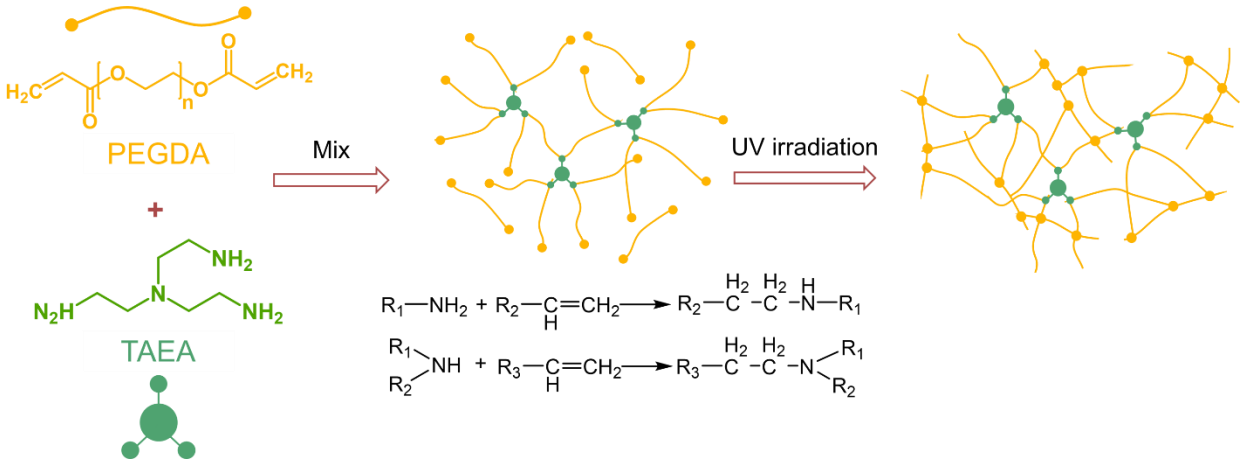

Scheme 1. Schematic representation of the two-stage procedure for preparing the cross-linked TAEA-PEGDA membrane.

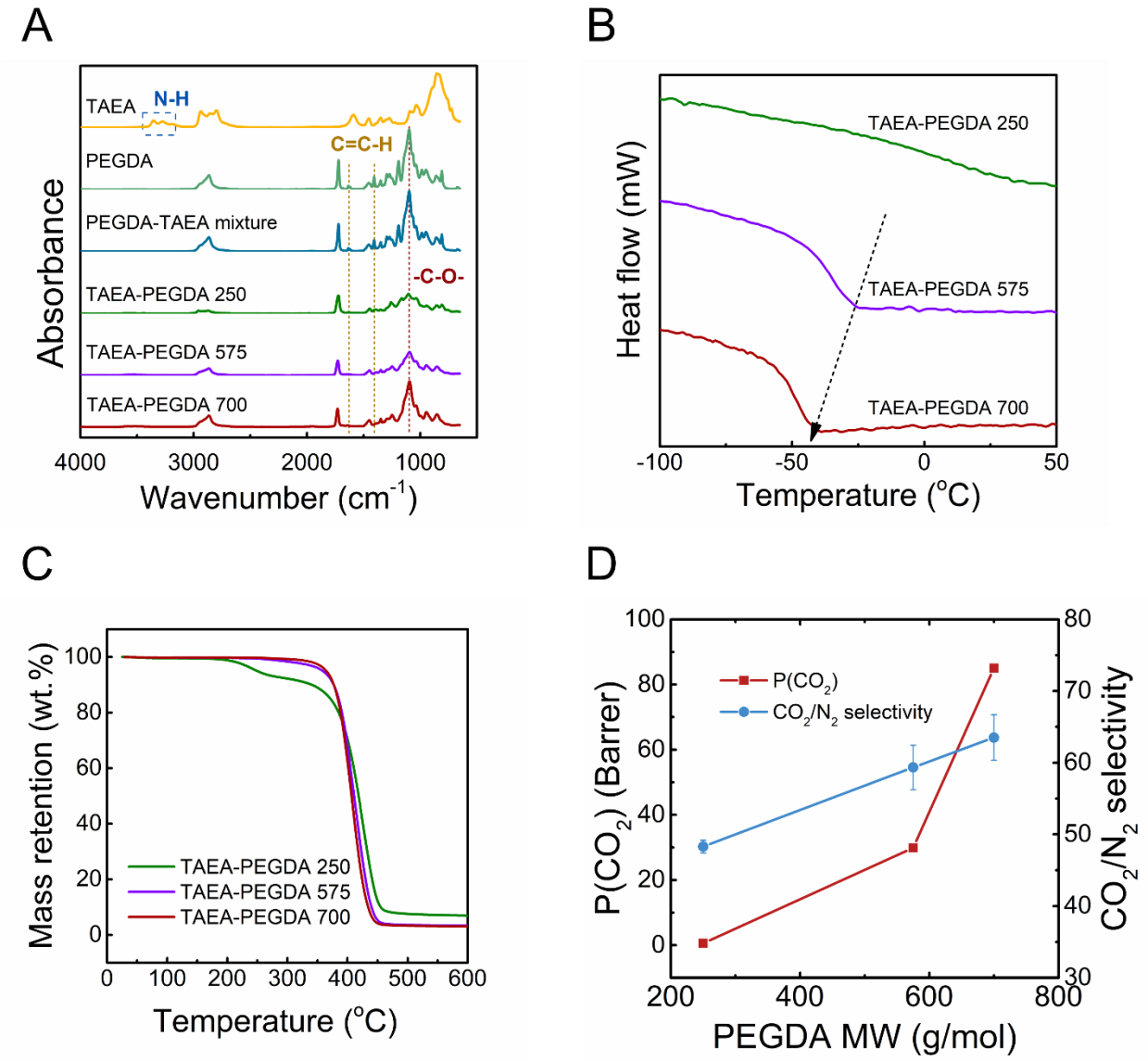

Figure 2. (A) FT-IR spectra, (B) DSC curves, (C) TGA results of PEGDA, TAEA and TAEA-PEGDA membranes, and (D) gas permeation results of TAEA-PEGDA membranes prepared by PEGDA of different MW (250, 575 and 700 g/mol) with the same N-H/acrylate ratio of 1:6.

According to the characterization results, it is clear that the PEGDA MW affects the properties of the resultant polymers. From the FT-IR spectra, the peak intensity of ether groups (around 1100 cm^{-1}) increases significantly with the increasing MW of PEGDA, which is reasonable since longer PEGDA contains more EO units. Fig. 2(B) shows that the glass transition temperature (T_g) of the resultant membranes decreases largely with the increasing PEGDA MW due to the longer and

more flexible polymer chains in the cross-linked membranes. The T_g of the membranes with PEGDA 250 is not observed in this work, which may be because of the highly restricted polymer chains caused by the high cross-linking density. Moreover, as shown in Fig.2 (C), membranes containing long PEGDA chains (PEGDA 575 and 700) possess good thermal stability with a one-step decomposition starting at ~ 360 ^{o}C, while the membrane with PEGDA 250 has a two-stage decomposition behavior and the first decomposition begins at ~ 200 ^{o}C due to the unreacted monomers. The reactions involving the short PEGDA chains (PEGDA 250) are extremely rapid, forming highly cross-linked polymer network that may block the further diffusion of the PEGDA 250 monomer, and thus some PEGDA 250 may stay as free monomer or form oligomers inside the polymer matrix.

The CO_2 and N_2 permeabilities of the resultant membranes were measured by single gas permeation tests, and the CO_2/N_2 ideal selectivity was calculated, as presented in Fig. 2 (D). It is worth mentioning that the error of the CO_2 permeability is very low (in most cases < 5 % of the average value), hence the error bars are almost invisible in the Fig. 2 (C). Detailed permeation data can be found in Table S1. As expected, the CO_2 permeability increases greatly (from 0.6 to 85 Barrer) with the increasing MW of PEGDA, consistent with the characterization analysis regarding the increasing free volume and CO_2 affinity of the membrane materials with the increase of the PEGDA MW. In addition, the increasing distance between the two cross-linking sites, because of the longer PEGDA monomer, results in looser cross-linking networks (lower cross-linking density), leading to a more permeable membrane. Furthermore, the increased ether content in the membrane of longer PEGDA monomers provides enhanced CO_2 affinity of the membrane and thus the improved CO_2 transport properties. This CO_2 permeation results are in agreement with Patel's work [9]. The CO_2/N_2 ideal selectivity also obtains notable increment (from 48.3 to 63.5), which is similar with the reported value of PEG-based material in the literature [2-4]. The increase in the CO_2/N_2 selectivity is believed contributed by the more ethylene units in the membrane matrix, as shown in the FT-IR results. Therefore, PEGDA 700 is chosen as the reactant monomer for further investigation.

3.2.Effect of N-H/acrylate ratio

The chemistry nature and the cross-linking density of the resultant membranes are tunable through changing the composition of the dual cross-linking networks (presented by the N-H bond/acrylate group ratio) [27, 28]. A higher N-H /acrylate ratio (N-H bond in TAEA to the acrylate in PEGDA) in the reactants implies that more TAEA will react with PEGDA and then less PEGDA will be left for the homo-polymerization step. Therefore, the effects of the N-H/acrylate ratio are investigated with regard to the network structure and thus membrane properties.

DSC, TGA, XRD, FI-IR, and gas permeation tests were performed to investigate the effects of the N-H/acrylate ratio on various properties of the resultant PEG-based polymers of interpenetrating networks from PEGDA700. Fig. 3 (A) presents the DSC curves of different N-H/acrylate ratios. As it can be seen, the T_g decreases with the increasing N-H/acrylate ratio, indicating enhanced chain mobility of the cross-linked polymers with increasing N-H/acrylate ratio. In addition, the TGA analysis (Fig. S1) shows that all TAEA-PEGDA700 membranes display sufficient thermal stability (T_{onset} > 200 ^oC) for most of the CO_2 separation applications. Most importantly, the XRD results (Fig. S2) suggest that the interpenetrating networks are amorphous according to the broad XRD peaks (at around 21^o) at all studied N-H/acrylate ratios, confirming that the tendency to become highly crystalline in PEG polymer has been suppressed. The FT-IR spectra of the membranes of different N-H/acrylate ratios are given in Fig. S3. Higher N-H/acrylate ratio means more C-N and less C-C bonds, which should be able to examine by FT-IR. However, the C-N has a similar frequency with C-C bonds in all cases. The FT-IR spectra of all TAEA-PEGDA700 membranes are nearly identical despite the different N-H/acrylate ratio. Nevertheless, at all N-H/acrylate ratio ratios, all amine and acrylate disappear in the FT-IR spectra of the membranes (Fig. S3), suggesting that both groups have fully reacted either in the aza-Michael reaction or in the acrylate homo-polymerization step in the membranes.

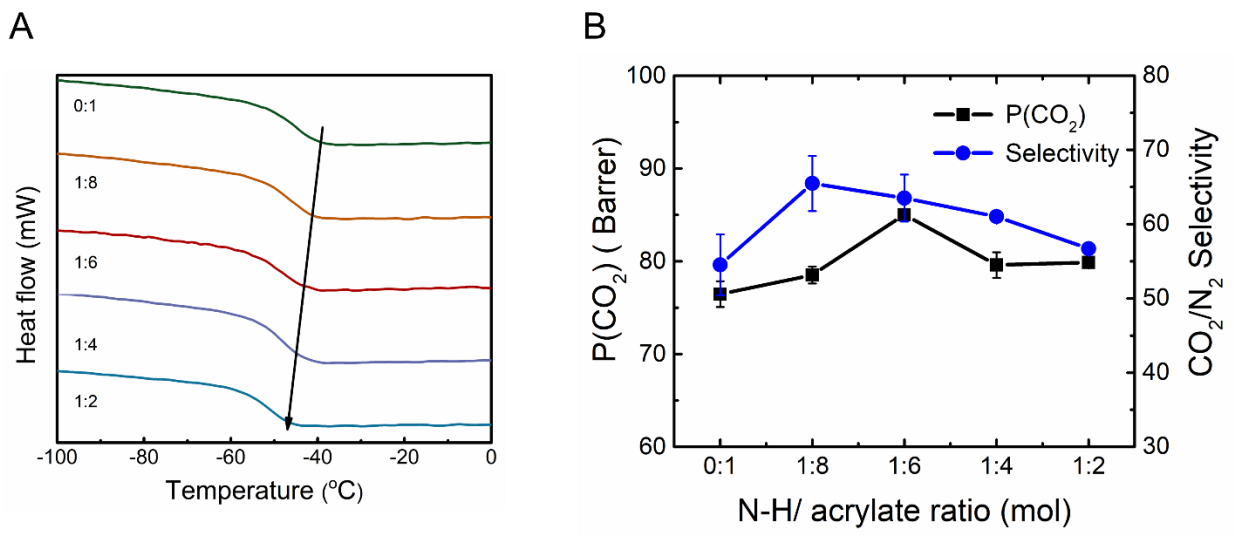

Figure 3. (A) The DSC results and (B) gas permeation results of TAEA-PEGDA700 membranes of different N-H/acrylate ratio.

The effect of N-H/acrylate ratio on CO_2 separation performance of the resultant membranes has been evaluated and the results are shown in Fig. 3 (B). The CO_2 permeability increases from 76.5 ± 1.4 to 85.0 ± 0.4 Barrer at the N-H/acrylate ratio of 1:6 and then maintains at a lower level of ~79 Barrer with a higher N-H/acrylate ratio. Similar trend is also observed in the CO_2/N_2 ideal selectivity: the selectivity increases from around 54.5 to 65.5 after adding a small amount of TAEA, and then decreases to 57 with further increasing N-H/ acrylate ratio, which is in the same range with the reported selectivity of PEG-based membranes (40-60) [4]. Theoretically, different cross-linking networks have different architecture structures and therefore different gas transport properties. However, the CO_2 permeability values of the membranes with N-H/acrylate of 0:1 and 1:1 are nearly the same, suggesting that the two networks have similar CO_2 transport properties despite the different network structures (star-like for TAEA-PEGDA network and parallel for pristine cross-linked PEGDA)[28]. This similar CO_2 permeation performance may be due to the rubbery nature of PEG chains and the same building unit PEGDA in both membranes. It is evident that the interpenetration of the chains affects the structure of both networks and results in more

free volume for gas transport, leading to the increased CO_2 permeability. On the other hand, the CO_2/N_2 selectivity of these membranes is not significantly influenced by changing the N-H/acrylate ratio. Hence, among the range of N-H / acrylate ratio studied in this work, the TAEA-PEGDA 700 membrane with an N-H / acrylate ratio of 1:6 was selected for further investigation due to its highest CO_2 permeability and higher CO_2/N_2 selectivity compared with the pristine cross-linked PEGDA. It is worth mentioning that the tertiary amine is the product of the aza-Michael addition used to build the interpenetrated network in the resultant membranes, which cannot function as CO_2 carriers due to the missing accessible N-H bonds and especially the absence of water vapor in the current test conditions.

3.3.IL blend membrane

In this work, four conventional ILs with different anions (i.e., [Bmim][BF_4], [Bmim][PF_6], [Bmim][TCM] and [Bmim][NTf_2]) were incorporated into the optimized cross-linked PEG-based membranes to study the influences of the IL addition on the membrane properties and the CO_2 separation performance. The FT-IR spectra of the pristine PEG membrane synthesized in this work and membranes containing four ILs (80 % ILs) are presented in Fig.4 (A). It is clear that there are peaks corresponding to their respective anion and the imidazole ring ($[Bmim]^+$) in all blend membranes. The information of related peaks are given as follows: 1051 cm^{-1} (B-F stretching of $[BF_4]^-$), 830 cm^{-1} (P-F stretching of $[PF_6]^-$), 2156 cm^{-1} (-C≡N stretching of $[TCM]^-$), 1181 cm^{-1} (C-F stretching of $[NTf_2]^-$) and 1571 cm^{-1} (C-C vibration of imidazole ring). It is also observed that the intensity of the aforementioned peaks are stronger than those related to the polymer chains in all IL blend membranes, which indicates a considerably high loading of ILs in the membrane matrix, suggesting that the cross-linked PEG membranes have the capability of possessing a high

amount ILs. In addition, with increasing ILs content, the peaks of ILs become more evident in the spectra of the blend membranes (Fig. S7), suggesting that the cross-linked PEG membrane networks have the capacity to contain a large amount of ILs. Compared with the cross-linked pristine PEGDA membrane (Fig. S6), different decomposition behaviors of the membranes containing ILs (i.e., starting point of decomposition and the decomposition rate) were observed, indicating the existence of the ILs inside the blend membranes.

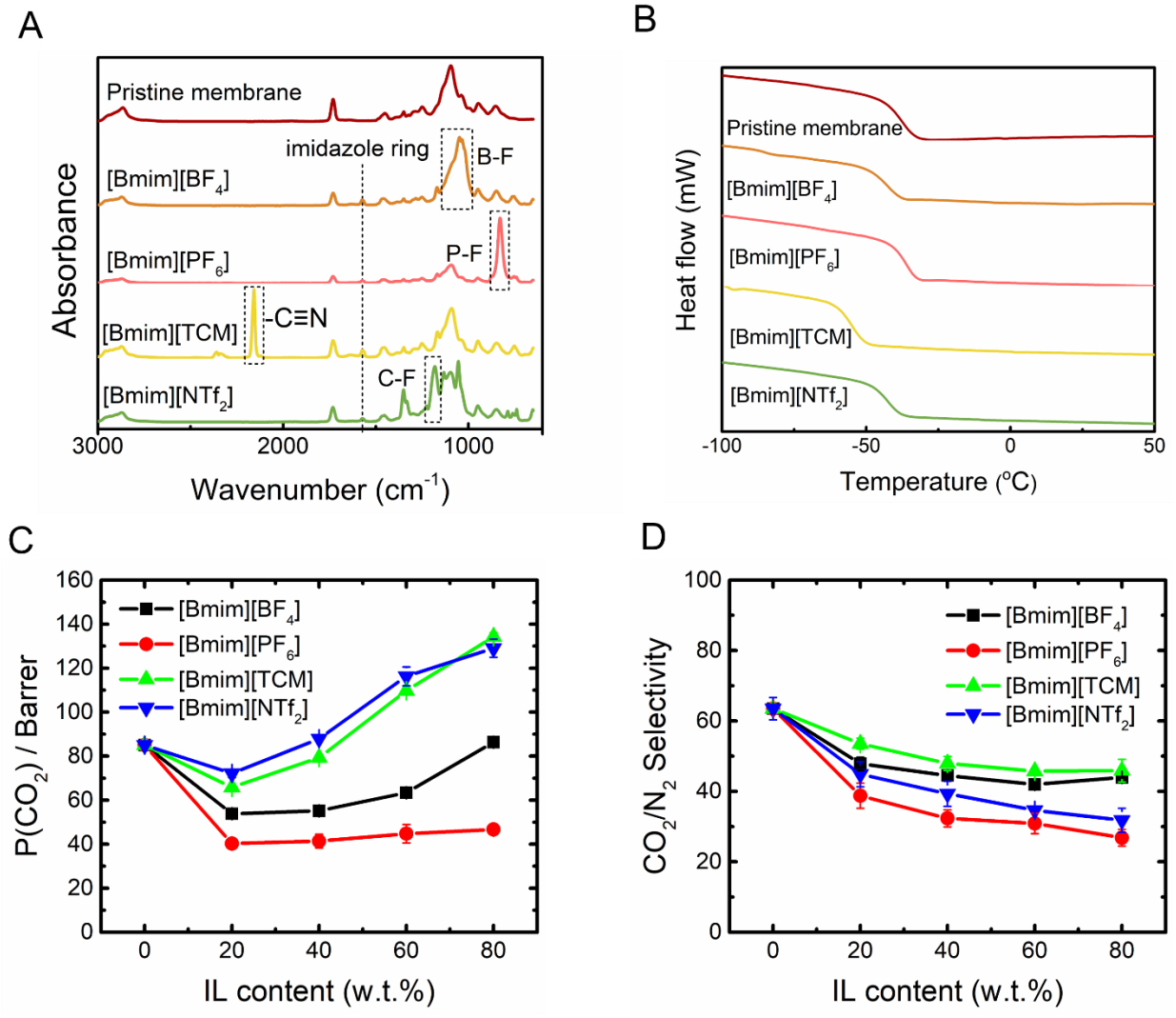

Figure 4. (A) The FT-IR spectra , (B) DSC curves of blend membranes with 80% IL loading, (C) CO_2 permeability and (D) CO_2/N_2 selectivity of four IL blend membranes with a function of ionic liquid content.

Generally speaking, T_g of a polymer decreases with adding low-molecular-weight additive into the polymer [3, 16], while a lower T_g usually indicates enhanced gas permeation properties. The T_g of the cross-linked PEG membranes incorporated with four selected ILs has been evaluated by DSC, as shown in Fig. 4(B). T_g of the membranes containing [Bmim][BF_4], [Bmim][TCM] and [Bmim][NTf_2] decreases with increasing IL content, indicating more flexible polymeric chains with the addition of ILs. In addition, the membranes containing different ILs show distinct values of T_g with the same IL loading (80 w.t.%): -57.1 °C, -58.9 °C, and -66.9 °C for membranes containing [Bmim][BF_4], [Bmim][NTf_2], and [Bmim][TCM], respectively, and -53.5 °C for the pristine membrane. This order is consistent with the values of the neat ILs. Additionally, only one T_g can be observed for each blend membrane, indicating the successful blending of ILs into the cross-linked PEG matrix. However, the trend of decreasing in T_g is less obvious in the membranes containing [Bmim][PF_6] compared with those with other ILs, as shown in Fig. S4, despite of the much lower T_g value of the neat IL. This difference may be ascribed to the intermolecular interactions, e.g., hydrogen bonding or Coulombic and van der Waals interactions between $[PF_6]^-$ and PEG polymer chains, which compensates the decreasing trend of T_g after adding ILs[29]. It is worth mentioning that the melting or crystallinity peaks of the four pure ILs are not observed in the spectra of the blend membranes, implying that ILs have been homogeneously mixed with the polymeric matrices. The incorporation of ILs into cross-linked PEG membranes also reduces its original crystallinity, proved by broader and less sharp peaks in XRD curves (Fig. S5).

The gas transport properties of the IL blend membranes have been measured by single gas permeation tests and the results are presented in Fig.4 (C). The CO_2 permeabilities of the membranes with four ILs decrease after adding a small amount of ILs (e.g., 20 wt. %), which may be because that ILs occupy the initial free volume of cross-linked PEG membranes, resulting in a decreased diffusivity and therefore lower permeability [30]. With more ILs added inside the membranes, CO_2 permeability increases with the IL loading except for [Bmim][PF_6]. For example, the membranes with 80 wt. % of [Bmim][TCM] has an around 2-fold increment in CO_2 permeability (134.2 Barrer) from the membrane with 20 wt. % IL content (65.8 Barrer). Several reasons could be responsible for the influence of the IL loading. Firstly, the presence of ILs during polymerization may lead to an increase in the free volume [11] and thus a higher gas diffusivity. Additionally, gases transport more easily through ILs than a solid polymer matrix and therefore permeate faster with more ILs inside the membranes. Moreover, the high affinity of ILs towards CO_2 enhances the CO_2 solubility, which also contributes to the increment of the CO_2 permeability.

Apparently, different ILs have different influences in the gas transport properties of the membranes. The cross-linked membranes with the addition of [Bmim][NTf_2] and [Bmim][TCM] show the highest CO_2 permeability, followed by that with [Bmim][BF_4], while the value of the membranes containing [Bmim][PF_6] locate in the bottom. The CO_2 permeability of the first two series of IL blend membranes is high as expected, as they are well-known for their good CO_2 absorption properties. But the enhancement of CO_2 permeability by the two ILs is believed by different mechanisms: the high affinity of $[NTf_2]^-$ to CO_2, mainly resulted by the plentiful fluoride atoms in the anion [31], may increase the CO_2 solubility, while the low viscosity of $[TCM]^-$ may have less transport resistance for CO_2 penetrating and hence an increased diffusivity [32]. For the case of [Bmim][BF_4], less fluorination in the anions leads to a lower Van der Waals force between the

anions and CO_2, thus a lower CO_2 solubility and permeability than $[NTf_2]^-$. Unexpectedly, the membranes containing $[PF_6]^-$ show a notable decrease in CO_2 permeability, even lower than that of the least CO_2-philic compound $[BF_4]^-$, which could be related to the interactions between $[PF_6]^-$ ions with the ethylene oxide groups.

It is worth mentioning that the CO_2/N_2 selectivity of these four ILs blend membranes decreases with the increasing ILs loading, as shown in Fig. 4 (D). This result is ascribed to the relatively lower CO_2/N_2 selectivity of these conventional ILs (20 ~ 30) compared with that of PEG-based materials (40 ~ 60). Therefore, the incorporation of conventional ILs into PEG-based materials show lower CO_2 selectivity. Different order has been observed for ideal CO_2/N_2 selectivity of the ILs blend membranes, which is $[TCM]^->[BF_4]^->[NTf_2]^->[PF_6]^-$. The highest selectivity of ILs blend membranes (45.9) comes from the high intrinsic CO_2/N_2 selectivity of cyanide-based anion, which is larger than that of the fluorinated ones [33, 34], and the more fluor groups ILs possess, the higher N_2 permeability and thus lower CO_2/N_2 selectivity membranes have [34]. Hence, the membrane with $[BF_4]^-$ have a greater selectivity than that with $[NTf_2]^-$ and the interactions between $[PF_6]^-$ and polymeric matrix results in the lowest selectivity.

4 Conclusion

In this work, four conventional ILs were incorporated in PEG-based membranes with interpenetrating networks based on aza-Michael addition and acrylate homo-polymerization. The study on the effect of MW of the monomer PEGDA on the material properties and CO_2 separation performance shows that longer PEGDA leads to better thermal stability and gas transport properties. The CO_2 permeability was around 144-time increment (from 0.6 to 85.0 Barrer) with a simultaneously increased CO_2/N_2 selectivity (from 48.3 to 63.5) when longer PEGDA is used (700

g/mol) instead of the short monomer (250 g/mol). The improvement in the CO_2 separation performance of the membranes is found the outcome of the increasing numbers of ethylene oxide units and more flexible polymer chains inside the membranes.

Membranes with varied N-H/acrylate ratio show different CO_2 separation performance. The CO_2 permeability increases and then decreases with the increasing N-H/acrylate ratio. The membrane with the best CO_2 separation performance is the one with N-H/acrylate of 1:6.

The incorporation of ILs improves the gas transport properties of the cross-linked PEG-based membranes by the enhanced CO_2 affinity from ILs. The CO_2 separation properties of the membrane changes with the addition of ILs and the changes depend on the content of ILs, which decreases with ILs addition at low loading (< 20 wt%) and then increases with the increasing ILs content. The addition of more CO_2-philic ILs leads to a higher CO_2 permeability in the order [Bmim][NTf_2] ≈ [Bmim][TCM] > [Bmim][BF_4]. The further addition of [Bmim][PF_6] into the membrane displays no increase in CO_2 permeation, hence the CO_2 permeability stays at a lower level compared with that of the pristine membrane. Although with a large increase in CO_2 permeability, a constant decrement in CO_2/N_2 selectivity was observed. The more CO_2-philic ILs, such as amine - functionalized ILs, may endow better CO_2 separation performance with higher CO_2 permeability and selectivity; this will be further studied.

ASSOCIATED CONTENTS

SUPPORTING INFORMATION

The TGA, FTIR, XRD results of TAEA-PEGDA700 membranes with different N-H ratio; the XRD, TGA and DSC results of the blend membranes with different ILs.

AUTHOR INFORMATION

Corresponding Author

* Liyuan Deng.

E-mail: deng@nt.ntnu.no, Tel.: +47 73594112,

ORCID:

Zhongde Dai: 0000-0002-3558-5403

Jing Deng: 0000-0003-3680-3799

Liyuan Deng: 0000-0003-4785-4620

Author Contributions

The manuscript was written through contributions of all authors. All authors have given approval to the final version of the manuscript.

Notes

The authors declare no competing financial interest.

Acknowledgments

This work was supported by the Research Council of Norway through the CLIMIT program (No. 254791).

REFERENCE

1. Hägg, M.-B.; Deng, L. Membranes in gas separation. In *Handbook of membrane separations: chemical, pharmaceutical, food, and biotechnological applications*, CRC Press: Boca Raton, FL, 2015; pp 143-180.
2. Wang, S.; Li, X.; Wu, H.; Tian, Z.; Xin, Q.; He, G.; Peng, D.; Chen, S.; Yin, Y.; Jiang, Z. Advances in high permeability polymer-based membrane materials for CO_2 separations. *Energy Environ. Sci.* **2016,** *9*, (6), 1863-1890.
3. Liu, J.; Hou, X.; Park, H. B.; Lin, H. High‐performance polymers for membrane CO_2/N_2 separation. *Chem. Eur. J.* **2016,** *22*, (45), 15980-15990.
4. Liu, S. L.; Shao, L.; Chua, M. L.; Lau, C. H.; Wang, H.; Quan, S. Recent progress in the design of advanced PEO-containing membranes for CO_2 removal. *Prog. Polym. Sci.* **2013,** *38*, (7), 1089-1120.
5. Kusuma, V. A.; Matteucci, S.; Freeman, B. D.; Danquah, M. K.; Kalika, D. S. Influence of phenoxy-terminated short-chain pendant groups on gas transport properties of cross-linked poly (ethylene oxide) copolymers. *J. Membr. Sci.* **2009,** *341*, (1-2), 84-95.
6. Wang, Y.; Li, H.; Dong, G.; Scholes, C.; Chen, V. Effect of Fabrication and Operation Conditions on CO_2 Separation Performance of PEO–PA Block Copolymer Membranes. *Ind. Eng. Chem. Res.* **2015,** *54*, (29), 7273-7283.
7. Lin, H.; Freeman, B. D. Gas solubility, diffusivity and permeability in poly (ethylene oxide). *J. Membr. Sci.* **2004,** *239*, (1), 105-117.
8. Lin, H.; Kai, T.; Freeman, B. D.; Kalakkunnath, S.; Kalika, D. S. The effect of cross-linking on gas permeability in cross-linked poly(ethylene glycol diacrylate). *Macromolecules* **2005,** *38*, (20), 8381-8393.
9. Patel, N. P.; Miller, A. C.; Spontak, R. J. Highly CO_2‐permeable and‐selective membranes derived from crosslinked poly (ethylene glycol) and its nanocomposites. *Adv. Funct. Mater.* **2004,** *14*, (7), 699-707.
10. Hirayama, Y.; Kase, Y.; Tanihara, N.; Sumiyama, Y.; Kusuki, Y.; Haraya, K. Permeation properties to CO_2 and N_2 of poly (ethylene oxide)-containing and crosslinked polymer films. *J. Membr. Sci.* **1999,** *160*, (1), 87-99.
11. Dai, Z.; Ansaloni, L.; Gin, D. L.; Noble, R. D.; Deng, L. Facile fabrication of CO_2 separation membranes by cross-linking of poly (ethylene glycol) diglycidyl ether with a diamine and a polyamine-based ionic liquid. *J. Membr. Sci.* **2017,** *523*, 551-560.
12. Yave, W.; Car, A.; Peinemann, K.-V. Nanostructured membrane material designed for carbon dioxide separation. *J. Membr. Sci.* **2010,** *350*, (1-2), 124-129.
13. Dai, Z.; Noble, R. D.; Gin, D. L.; Zhang, X.; Deng, L. Combination of ionic liquids with membrane technology: A new approach for CO_2 separation. *J. Membr. Sci.* **2016,** *497*, 1-20.
14. Bara, J. E.; Noble, R. D.; Gin, D. L. Effect of "Free" Cation Substituent on Gas Separation Performance of Polymer−Room-Temperature Ionic Liquid Composite Membranes. *Ind. Eng. Chem. Res.* **2009,** *48*, (9), 4607-4610.
15. Chen, H. Z.; Li, P.; Chung, T.-S. PVDF/ionic liquid polymer blends with superior separation performance for removing CO_2 from hydrogen and flue gas. *Int. J. Hydrogen Energy* **2012,** *37*, (16), 11796-11804.
16. Dai, Z.; Bai, L.; Hval, K. N.; Zhang, X.; Zhang, S.; Deng, L. Pebax®/TSIL blend thin film composite membranes for CO_2 separation. *Sci. China. Chem.* **2016,** *59*, (5), 538-546.
17. Dai, Z.; Ansaloni, L.; Ryan, J. J.; Spontak, R. J.; Deng, L. Nafion/IL hybrid membranes with tuned nanostructure for enhanced CO_2 separation: effects of ionic liquid and water vapor. *Green Chem.* **2018,** *20*, (6), 1391-1404.

18. Kusuma, V. A.; Macala, M. K.; Baker, J. S.; Hopkinson, D. Cross-Linked Poly(ethylene oxide) Ion Gels Containing Functionalized Imidazolium Ionic Liquids as Carbon Dioxide Separation Membranes. *Ind. Eng. Chem. Res.* **2018,** *57*, (34), 11658-11667.
19. Gao, H.; Bai, L.; Han, J.; Yang, B.; Zhang, S.; Zhang, X. Functionalized ionic liquid membranes for CO_2 separation. *Chem. Commun.* **2018,** *54*, (90), 12671-12685.
20. Deng, J.; Bai, L.; Zeng, S.; Zhang, X.; Nie, Y.; Deng, L.; Zhang, S. Ether-functionalized ionic liquid based composite membranes for carbon dioxide separation. *RSC Adv.* **2016,** *6*, (51), 45184-45192.
21. Zhou, J.; Mok, M. M.; Cowan, M. G.; McDanel, W. M.; Carlisle, T. K.; Gin, D. L.; Noble, R. D. High-permeance room-temperature ionic-liquid-based membranes for CO_2/N_2 separation. *Ind. Eng. Chem. Res.* **2014,** *53*, (51), 20064-20067.
22. Bara, J. E.; Hatakeyama, E. S.; Gabriel, C. J.; Zeng, X.; Lessmann, S.; Gin, D. L.; Noble, R. D. Synthesis and light gas separations in cross-linked gemini room temperature ionic liquid polymer membranes. *J. Membr. Sci.* **2008,** *316*, (1), 186-191.
23. Bara, J. E.; Hatakeyama, E. S.; Gin, D. L.; Noble, R. D. Improving CO_2 permeability in polymerized room-temperature ionic liquid gas separation membranes through the formation of a solid composite with a room-temperature ionic liquid. *Polym. Adv. Technol.* **2008,** *19*, (10), 1415-1420.
24. Zeng, S.; Zhang, X.; Bai, L.; Zhang, X.; Wang, H.; Wang, J.; Bao, D.; Li, M.; Liu, X.; Zhang, S. Ionic-liquid-based CO_2 capture systems: structure, interaction and process. *Chem. Rev.* **2017,** *117*, (14), 9625-9673.
25. Kusuma, V. A.; Macala, M. K.; Liu, J.; Marti, A. M.; Hirsch, R. J.; Hill, L. J.; Hopkinson, D. Ionic liquid compatibility in polyethylene oxide/siloxane ion gel membranes. *J. Membr. Sci.* **2018,** *545*, 292-300.
26. Bernardo, P.; Jansen, J. C.; Bazzarelli, F.; Tasselli, F.; Fuoco, A.; Friess, K.; Izák, P.; Jarmarová, V.; Kačírková, M.; Clarizia, G. Gas transport properties of Pebax®/room temperature ionic liquid gel membranes. *Sep. Purif. Technol.* **2012,** *97*, 73-82.
27. González, G.; Fernández-Francos, X.; Serra, À.; Sangermano, M.; Ramis, X. Environmentally-friendly processing of thermosets by two-stage sequential aza-Michael addition and free-radical polymerization of amine–acrylate mixtures. *Polym. Chem.* **2015,** *6*, (39), 6987-6997.
28. Deng, J.; Dai, Z.; Yan, J.; Sandru, M.; Sandru, E.; Spontak, R. J.; Deng, L. Facile and solvent-free fabrication of PEG-based membranes with interpenetrating networks for CO_2 separation. *J. Membr. Sci.* **2019,** *570-571*, 455-463.
29. Trivedi, S.; Pandey, S. Interactions within a [Ionic Liquid + Poly(ethylene glycol)] Mixture Revealed by Temperature-Dependent Synergistic Dynamic Viscosity and Probe-Reported Microviscosity. *J. Phys. Chem. B* **2011,** *115*, (22), 7405-7416.
30. Kanehashi, S.; Kishida, M.; Kidesaki, T.; Shindo, R.; Sato, S.; Miyakoshi, T.; Nagai, K. CO_2 separation properties of a glassy aromatic polyimide composite membranes containing high-content 1-butyl-3-methylimidazolium bis (trifluoromethylsulfonyl) imide ionic liquid. *J. Membr. Sci.* **2013,** *430*, 211-222.
31. Lei, Z.; Dai, C.; Chen, B. Gas Solubility in Ionic Liquids. *Chem. Rev.* **2014,** *114*, (2), 1289-1326.
32. Kim, J. E.; Kim, H. J.; Lim, J. S. Solubility of CO_2 in ionic liquids containing cyanide anions:$[C_2mim][SCN]$, $[C_2mim][N(CN)_2]$ and $[C_2mim][C(CN)_3]$. *Fluid Phase Equilib.* **2014,** *367*, 151-158.
33. Scovazzo, P.; Kieft, J.; Finan, D. A.; Koval, C.; DuBois, D.; Noble, R. Gas separations using non-hexafluorophosphate $[PF6]^-$ anion supported ionic liquid membranes. *J. Membr. Sci.* **2004,** *238*, (1), 57-63.
34. Mahurin, S. M.; Lee, J. S.; Baker, G. A.; Luo, H.; Dai, S. Performance of nitrile-containing anions in task-specific ionic liquids for improved CO_2/N_2 separation. *J. Membr. Sci.* **2010,** *353*, (1), 177-183.

TOC

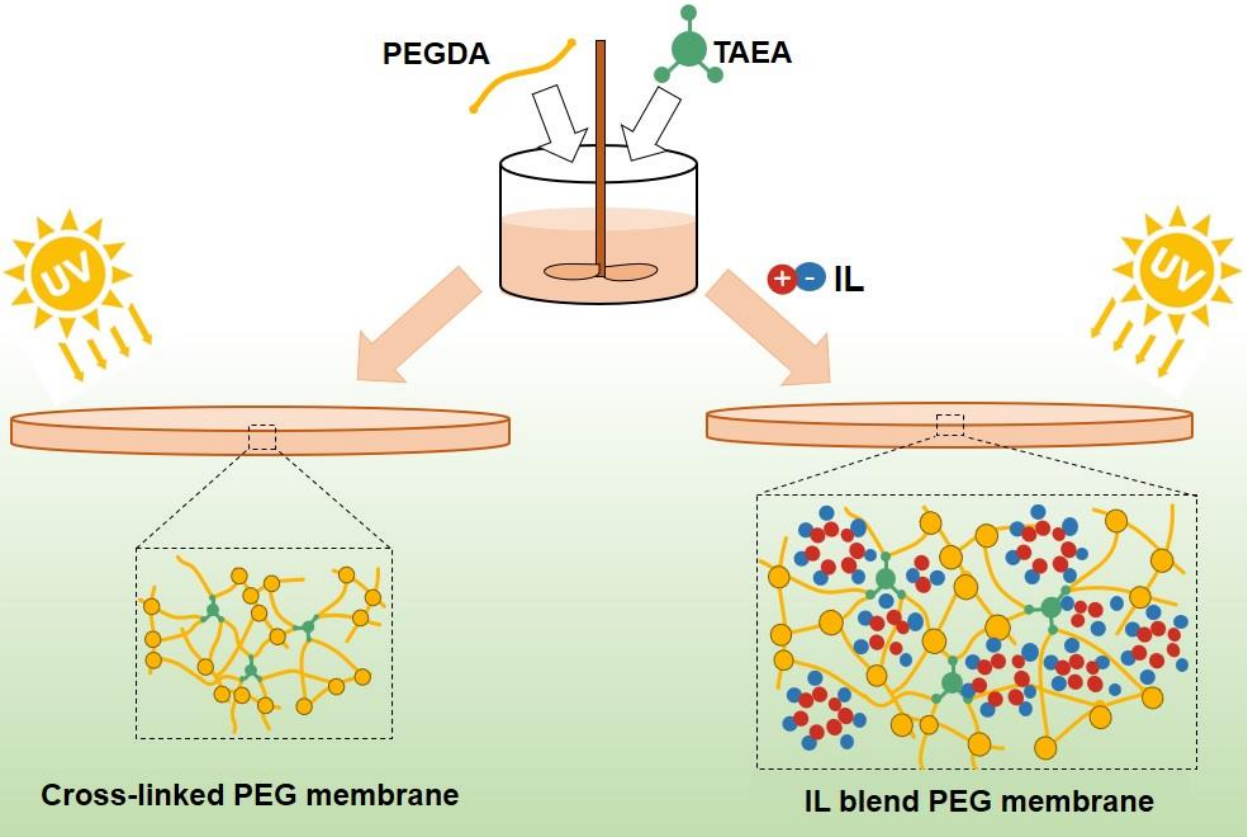
PEGDA
TAEA
IL
UV
UV
Cross-linked PEG membrane
IL blend PEG membrane